JOURNAL OF AERONAUTICS AND SPACE TECHNOLOGIES
(ISSN : 1304-0448)
July 2020 Volume 13 Number 2
www.jast.hho.edu.tr

Research Article

Clutter Learning Based LS Method for Buried Target Detection in GPR Images

Deniz KUMLU[1], Işın ERER[2]

[1] *National Defense University, Turkish Naval Academy, Electrical and Electronics Department, 34942 Tuzla , Istanbul, Turkey,* dkumlu@dho.edu.tr, https://orcid.org/0000-0002-7192-7466

[2] *Istanbul Technical University, Electrical and Communication Engineering Department, 34469 Maslak, Istanbul, Turkey,* ierer@itu.edu.tr, https://orcid.org/0000-0002-2225-6379

Article Info

Received: *May 16, 2020*
Accepted: *July 11, 2020*
Online: *July 27, 2020*

Keywords: Least squares, Regularized least squares, Clutter learning, GPR, gprMax, RPCA

Abstract

A regularized version of the least squares (LS) target detection method is combined with the subspace-based clutter learning for buried target detection in ground penetrating radar (GPR) images. The LS method is used to estimate the next A-scans from previously observed A-scans which are assumed to belong to the clutter component. Generally, A-scans used in the initial stage are accepted as target-free for the LS to work correctly. However, this is not guaranteed and if the first observed A-scan samples contain any target information, LS method will fail. In this paper, the clutter information is retrieved via robust principal component analysis (RPCA) as a preprocessing stage and used in the LS estimation of the actual A-scan. Thus, for A-scans containing target information, LS method will provide an increase in the estimation error indicating target presence at this location. Moreover, due to the regularization, the proposed method is more robust to noise caused by the irregularities of the soil.

To Cite This Article: D. Kumlu, I. Erer, "Clutter Learning Based LS Method for Buried Target Detection in GPR Images", Journal of Aeronautics and Space Technologies, Vol. 13, No. 2, pp. 217-225, July 2020.

YNR Görüntülerinde Gömülü Hedef Tespitini için Kargaşa Öğrenme Tabanlı LS Metodu

Makale Bilgisi

Geliş: *16 Mayıs 2020*
Kabul: *11 Temmuz 2020*
Yayın: *27 Temmuz 2020*

Anahtar Kelimeler: En küçük kareler, Düzenlileştirilmiş en küçük karaler, Kargaşa öğrenme, YNR, gprMax, GTBA

Öz

En küçük kareler (EKK) hedef tespit yönteminin düzenleştirilmiş versiyonu ile alt uzay tabanlı kargaşa giderme, yere nüfuz eden radar (YNR) görüntülerinde gömülü hedef tespiti için birleştirilmiştir. EKK yöntemi geçmişte gözlenmiş A-taramaları kullanarak, gelecek A-taramayı tahmin etmeye çalışır ve gözlemlenmiş A-taramanın kargaşa bileşenine ait olduğu varsayımı mevcuttur. Genellikle, EKK'nin doğru çalışabilmesi için, başlangıç aşamasında gözlemlenen A-taramalarda hedefe ait olmadığı kabul edilir. Fakat bu her zaman doğru bir varsayım değildir ve ilk gözlemlenen A-taramalarda hedef bileşeni mevcutsa, EKK yöntemi başarısız olacaktır. Bu çalışmada, ön adım olarak kargaşa bilgisi gürbüz temel bileşen analizi (GTBA) yöntemi ile çıkartılmıştır ve bu bilgi EKK'nin gelecek A-taramayı tahmini için kullanılmıştır. Böylece, hedef bilgisi içeren A-taramalarda EKK yönteminin tahmin hatası artacağından, bu A-taramalarda bölgesinde hedefin olduğunu gösterecektir. Ayrıca, düzenlileştirme işleminden dolayı, önerilen yöntem yüzey düzensizliklerinden dolayı meydana gelen gürültüye karşı daha gürbüz olacaktır.

1. INTRODUCTION

Ground-penetrating radar (GPR) is a popular tool for buried object detection and has various applications in both civilian and military areas. It is generally preferred for the detection of non-metallic and plastic buried objects and achieves high detection rates. Its working principle is based on sending and receiving electromagnetic pulses. For a given antenna location, the collected signal is called as A-scan. GPR is moved on a

line by uniform distances to scan a desired area and concatenation of the collected A-scans from corresponding each antenna locations constitute the B-scan or the GPR image [1].

However, the detection performance of GPR algorithms can be highly affected by the clutter caused by direct-wave arrival, ground bounce, other candidate buried objects and electromagnetic properties of the buried environment. The obtained GPR image basically contains the clutter and target components together. Most of the detection methods try to model the clutter by assuming that the first observed A-scans in the GPR image belong to the clutter component [2-4]. However, this is a very weak assumption since the target or targets can be found anywhere. If the first observed A-scans used to model the clutter contain any target information, the detection performance will decline considerably.

In this paper, we propose a two-stage detection algorithm composed of clutter learning and target detection stages. First the clutter component of the input GPR image is obtained via a subspace-based method, namely Robust Principal Component (RPCA) [5] then, all the A-scans in the input GPR image are compared with the learned clutter component. An anomaly in the error plots indicates a target presence at the corresponding location. Clutter learning stage provides an opportunity to use only the clutter information of the GPR image in the detection stage.

Subspace-based methods [6]-[10] such as singular value decomposition (SVD) [7]-[9], principal component analysis (PCA) [7]-[9], independent component analysis (ICA) [7]-[9] as well as recently proposed non-negative matrix factorization (NMF) [10] and robust principal component analysis (RPCA) [5], [11], [12] can be used for clutter removal purposes in GPR images. The SVD, PCA, ICA and recently proposed NMF are known as low-rank approximation methods and decompose the GPR image into clutter and target components by using different matrix decomposition constraints. Recently proposed NMF provides a low rank approximation of GPR data which corresponds to the clutter component. The recently proposed RPCA method provides a sparse part alongside the low-rank part. In RPCA decomposition of the GPR image, the clutter corresponds to the low-rank component and the target corresponds to the sparse component. RPCA method has superior results compared to the conventional subspace-based methods such as SVD, PCA, ICA and NMF. In our method, learning the clutter part of the GPR image is crucial in the preprocessing step. If the clutter part is learned well enough, the performance of the detection method will also increase. On the other hand, since they are fast enough, using clutter learning methods as a preprocessing step of the detection algorithm does not cause extra computational complexity.

Least Squares (LS) is a very popular method in statistics [13] and which has found many applications in image processing. In GPR, LS uses previous A-scans to estimate the next A-scans and previous A-scans are assumed to belong to the clutter part for LS to work correctly [2]. If this assumption fails, then LS gives false alarms. Our proposed method eliminates this issue by obtaining only the clutter part of the GPR image. Therefore, we guarantee that the previously observed A-scans carry only the clutter information. After that, the classical LS method approach can be applied to the next A-scans [14]. However, it is known that classical LS solution deteriorates when the correlation matrix of the observed data is ill-conditioned (its determinant is close to zero) which is common for noisy measurements. In this paper, we also propose a regularized LS (regLS) solution where LS solution is penalized with *L2- norm* of the unknown vector. Thus our original contributions may be cited as clutter learning as a preprocessing step and a regularized LS detector.

The rest of the paper is organized as follows. In section 2, we review the LS based target detection method. Section 3 presents a proposed two-stage detection method which includes decomposition stage via RPCA and a regularized version of LS based target detection method. Section 4 presents the results for both simulated and real scenarios. Concluding remarks are given in section 5.

2. BURIED TARGET DETECTION WITH LS METHOD

Let $X \in \mathbb{R}^{M \times N}$ represent the GPR data matrix where M denotes the depth or time of the GPR image while N represents the number of A-scans or antena location information.

$$X = \begin{bmatrix} x_{1,1} & \dots & x_{1,N} \\ \vdots & \ddots & \vdots \\ x_{M,1} & \dots & x_{M,N} \end{bmatrix} \quad (1)$$

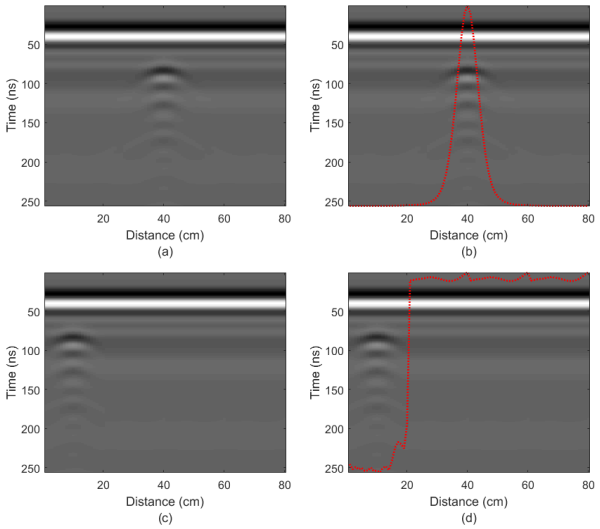

Figure 1. Sample raw GPR image with (a) target located in the middle, (b) LS detection result, (c) target located in the beginning, (d) LS detection result.

It is possible to estimate a given A-scan at location *i*, $\mathbf{x}_i = [x_{i,1} \quad \dots \quad x_{i,N}]$ from previously observed A-scans as [2]

$$y = wX_i \tag{2}$$

where $w \in \mathbb{R}^{K\times K}$ is the filter coefficients, K is the previously observed A-scans vector and $y \in \mathbb{R}^{M\times 1}$ is the least square estimation and X_i is the matrix representing

$$X_i = \begin{bmatrix} x_{1,i-K+1} & \dots & x_{1,i-1} \\ \vdots & \ddots & \vdots \\ x_{M,i-K+1} & \dots & x_{M,N} \end{bmatrix} \tag{3}$$

The estimation error is given as

$$e = d - y \tag{4}$$

where $d \in \mathbb{R}^{M\times 1}$ denotes the desired signal.

The LS solution is obtained by minimizing $e \in \mathbb{R}^{M\times 1}$ and can be given as:

$$R\hat{w} = p \tag{5}$$

where $\hat{w}$ corresponds to optimum filter coefficients with $R = X_i^T X_i$ and $p = X_i^T y$. Therefore, (5) can be written as

$$\hat{w} = R^{-1}p \tag{6}$$

by using the optimum filter coefficients in (6), the least square estimation can be calculated by (2) and the estimation error can be found from (4) [2].

Figure 1(a)-(d) show GPR images and the error or anomaly plots (red line) provided by the LS method for two different cases: in the first row, the buried target is in the middle (of the GPR image) as it is generally assumed and in the second row the buried target is in the first A-scans. The peak of the error plot indicates the target location or anomaly locations. In Figure 1(b) anomaly locations correspond to target location, since the conventional LS method uses the first A-scans to model the clutter. However, in the second case the target is present in the first A-scans as shown in Figure 1(c) and LS fails to detect the target location as shown in Figure 1 (d). Thus, the general assumption [2] fails in this scenario.

3. PROPOSED METHOD

3.1. Clutter Learning Step

The raw GPR image can be considered as a mixed image composed of clutter and target components which can be recovered by classical low rank based approximations such as SVD, PCA, ICA [7-9] or the recently proposed RPCA based clutter removal method [5].

RPCA provides a low rank matrix $L \in \mathbb{R}^{M\times N}$ and sparse matrix $S \in \mathbb{R}^{M\times N}$ decomposition for a given input GPR image [15]. Thus, the rectangular GPR image $X \in \mathbb{R}^{M\times N}$ can be represented as

$$X = L + S \tag{7}$$

The decomposition problem in (7) can be solved by the following optimization problem formulated as

$$\min_{L,S} \|L\|_* + \lambda\|S\|_1 \quad \text{subject to} \quad |X - (L+S)| \le \varepsilon \tag{8}$$

In (8), the low rank part L can be obtained by the minimization of $\|L\|_*$, the nuclear form of L (the sum of singular values). $\|S\|_1$ which denotes l-1 norm of S, is defined as the sum of the entries in S, λ is the penalization parameter between L and S and ε is the error matrix to improve the convergence. L and S are given by successive SVD thresholding operations followed by the soft-thresholding of the residual matrices [15].

After the decomposition of the GPR image with RPCA, the low rank matrix L corresponds to the clutter part and the sparse matrix S corresponds to the target part.

3.2. Target Detection Step

In the classical LS based target detection method, it is assumed that the previously observed first 5, 10 or 15 A-scans of the GPR image belong only to the clutter part.

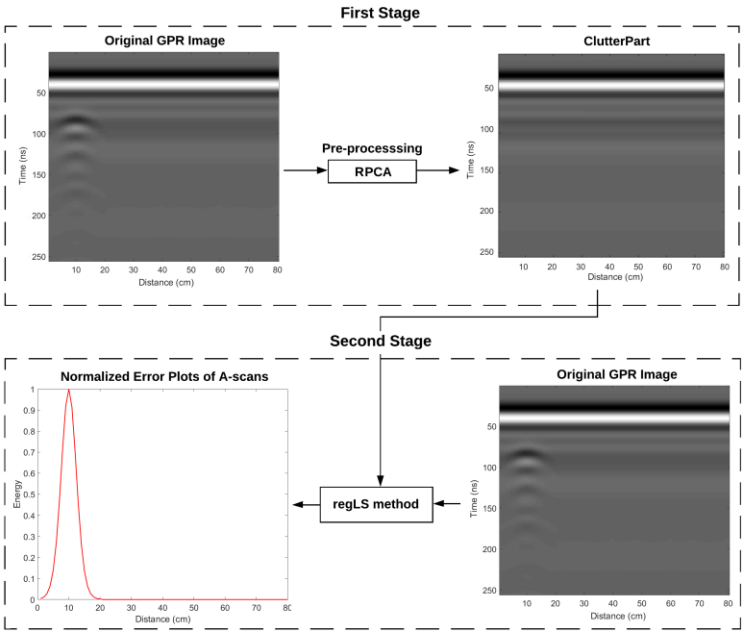

Figure 2. The two-stage block diagram of the proposed LS-based target detection.

Then, LS method uses them to model the clutter. Each following A-scan is compared with the model containing the clutter information and the error between the estimated and actual A-scans is calculated. If the error is higher than a predefined threshold, it is assumed that there is an anomaly (target presence) at this location [2].

In the LS based target detection method, if the input GPR image is similar to the one shown in the Figure 1(a) where the first previously observed A-scans belong only to the clutter part, LS will work successfully. However, if the initial A-scans contain target information as in the Figure 1(c), the LS method will use A-scans which also contain target information, leading to deteriorated detection results.

In this study, we propose a two-stage algorithm to avoid the risk defined above for GPR images with scenarios similar to Figure 1(c). The first part of the method can be accepted as a preprocessing stage where the clutter part of the input GPR image is estimated. Then, this information is used as an input to LS method to model the A-scans that belong to the clutter. Finally, the modeled A-scans are compared with the next observed A-scans and the modelling errors are obtained.

The diagram of the proposed method is shown in Figure 2. As seen in Figure 2, the error plot provided by the proposed method shows the exact location of the buried target. However, the LS method may be affected from slight modifications of the measurement data or there may be a singularity problem during the matrix inversion, thus one may prefer to use a *L2-norm* regularized version [16] obtained by minimizing

$$min_w \|y - Xw\|_2 + \lambda \|w\|_2 \tag{9}$$

A closed-form solution of (9) is given as

$$\hat{w} = (X^T X + \lambda I)^{-1} X^T y \tag{10}$$

where $I \in \mathbb{R}^{K \times K}$ corresponds to the identity matrix.

The stages of the proposed method are given in Figure 2. The GPR image is decomposed by RPCA into its low-rank L (clutter) and sparse S (target) components [5]. The L component is used in the regLS to estimate i^{th} A-scan. If the estimation error exceeds a predefined level, a target decision is made for this location.

4. SIMULATED AND EXPERIMENTAL RESULTS

In the experimental part, two experiments are conducted to validate the performance of our proposed method. In the first experiment, the simulated dataset is generated by the gprMax simulation software tool. Receiver operating characteristic (ROC) curves are used for quantitative analysis.

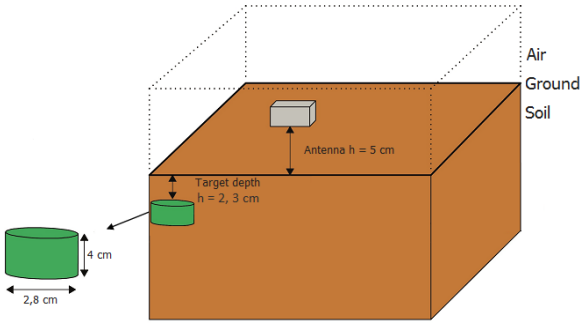

Figure 3. Experimental design of the simulated dataset.

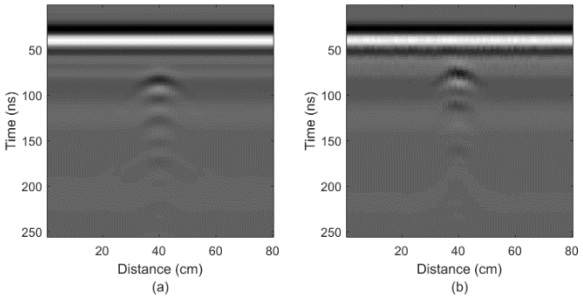

Figure 4. Sample raw GPR image from our simulated dataset a) flat and b) rough ground.

We first tested the clutter removal performance of classical low rank and the recently proposed RPCA based clutter removal methods to show the superiority of RPCA. Then, we proceed with the RPCA for the clutter learning step in our proposed method. In the second experiment, a real dataset is used. The field tests are important to evaluate the performance of the results. However, since the real dataset contains a limited number of images and scenarios, instead of ROC analysis which require a large number of GPR images, energy plots are provided.

Table 1. Electromagnetic properties of the materials.

Material	$D.C.\ (F/m)$	$C.\ (S/m)$
Dry sand	3.0	0.001
Damp sand	8.0	0.01
Wet sand	20.0	0.1
Dry clay soil	10.0	0.01
Wet clay soil	12.0	0.01
Dry loam soil	10.0	0.001
Aluminum	3.1	2.3e7
Plastic	3.0	0.01

4.1. Simulated Dataset Results

Our simulated dataset produced using the gprMax simulation software program [17]. In newest version of the gprMax, different soil types, various type of buried materials with different dimensions, different burial depths and various surface types can be modeled. Our simulated dataset contains 112 images of 7 different soil types, 2 different materials, 2 different burial depths and 4 different surface types [8]. The setup of the scenario fort he simulated dataset is shown in Figure 3. The electromagnetic properties of the different soil types and materials are given in Table 1.

The first stage contains the decomposition of GPR image into clutter and target components. To show the superiority of RPCA [5] as a clutter removal method, it is compared with the low rank based methods both visually and quantitatively. The obtained results are shown in Figure 5 (a)-(e) and Figure 6 (a)-(e) which belong to Figure 4 (a) and (b), raw GPR images of flat and rough ground surface, respectively. The visual results in Figure 5 (a)-(e) show the clutter and target components by using different decomposition methods for the flat ground raw GPR image (simple scenario). The low rank based methods (SVD, PCA, ICA) show some distortion in the target part and some undesired horizontal lines are observed in both clutter and target components. However, the RPCA result shown in Figure 5 (e) is quite clear and there is no remaining clutter component in the target part, validating the superiority of RPCA compared to the other clutter removal methods.

The decomposition results in Figure 6 (a)-(e) show the clutter and target component for the rough ground surface for raw GPR image in Figure 4 (b) (difficult scenario). Since, the surface type is rough, which is common in field tests, decomposition results are not satisfactory. PCA and ICA methods show some distortion in the target component and this also affects the clutter component naturally since the raw GPR image is the sum of the two components. The results of SVD and NMF are similar however they both contain some clutter on the surface and present some horizontal lines. The result of RPCA is quite smooth and there is less surface clutter on the target component. Therefore, it can be concluded that RPCA shows the best decomposition results while the PCA and ICA present the worst results.

The superiority of RPCA is also demonstrated in the ROC curves as given in Figure 7. The performance of NMF is slightly better than the SVD method while PCA and ICA have the worst performance among all. Thus we used RPCA for clutter learning step in the following sections.

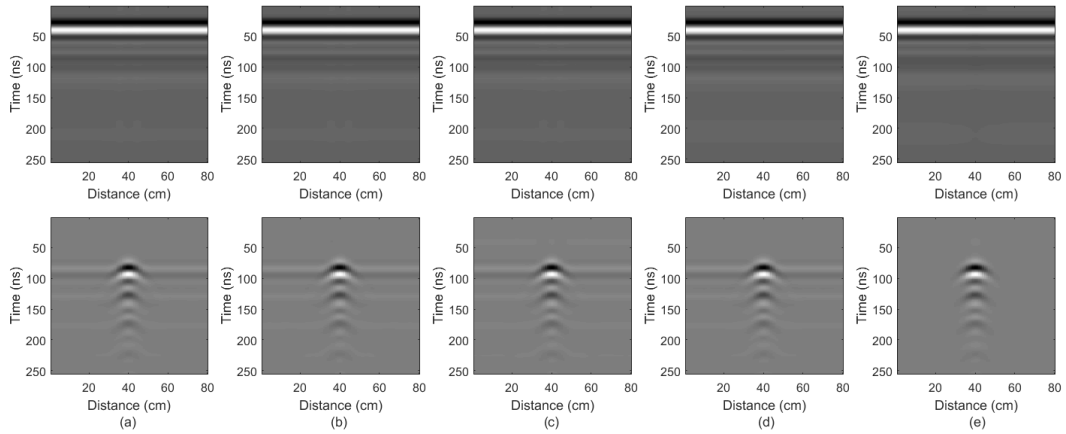

Figure 5. The results of the raw GPR image decomposition methods (first row clutter, second row target component) for flat surface ground a) SVD b) PCA c) ICA d) NMF e) RPCA.

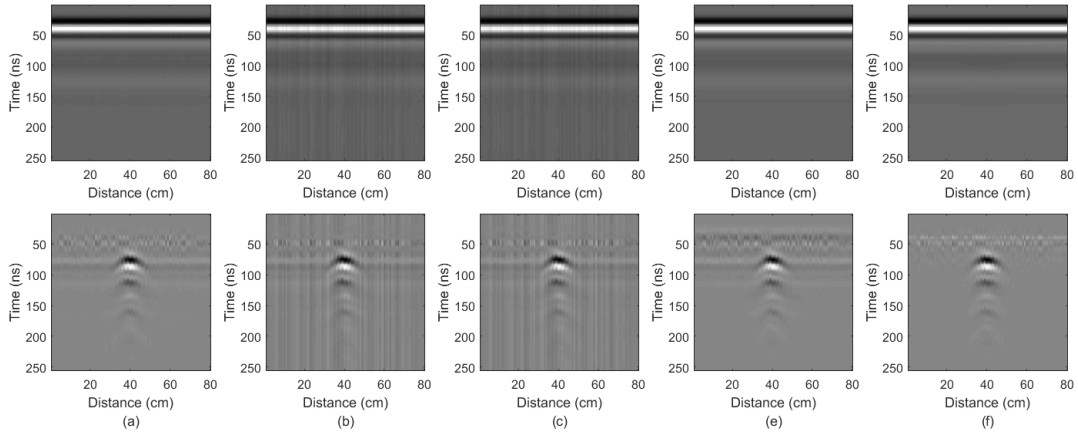

Figure 6. The results of the raw GPR image decomposition methods (first row clutter, second row target component) for rough surface ground a) SVD b) PCA c) ICA d) NMF e) RPCA.

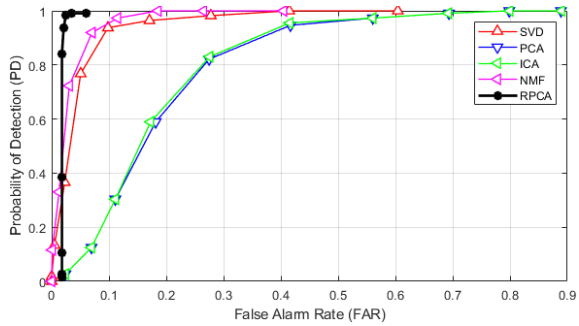

Figure 7. ROC curves comparison of the GPR data decomposition methods.

The clutter information provided by RPCA, is used in both LS and regLS estimations. The ROC analysis in Figure 8 shows that the classical LS method, the regLS (without any clutter removal), LS_{RPCA} and $regLS_{RPCA}$ (with clutter removal by RPCA) methods are compared for the simulated dataset.

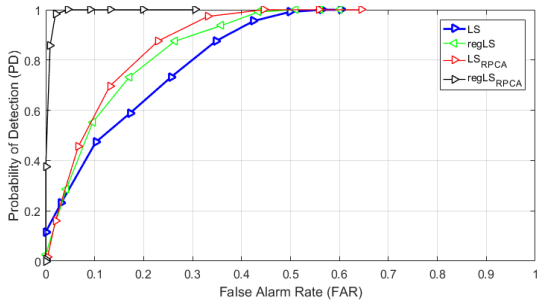

Figure 8. ROC curves comparison of the target detection methods for simulated dataset.

As expected, using the regularized version of LS enhances the detection performance compared to the classical LS. It can be observed that LSR_{RPCA} and $regLS_{RPCA}$ based methods outperform LS and regLS since the clutter information is used. A slight improvement in the detection performance is observed for regLs compared to the LS method.

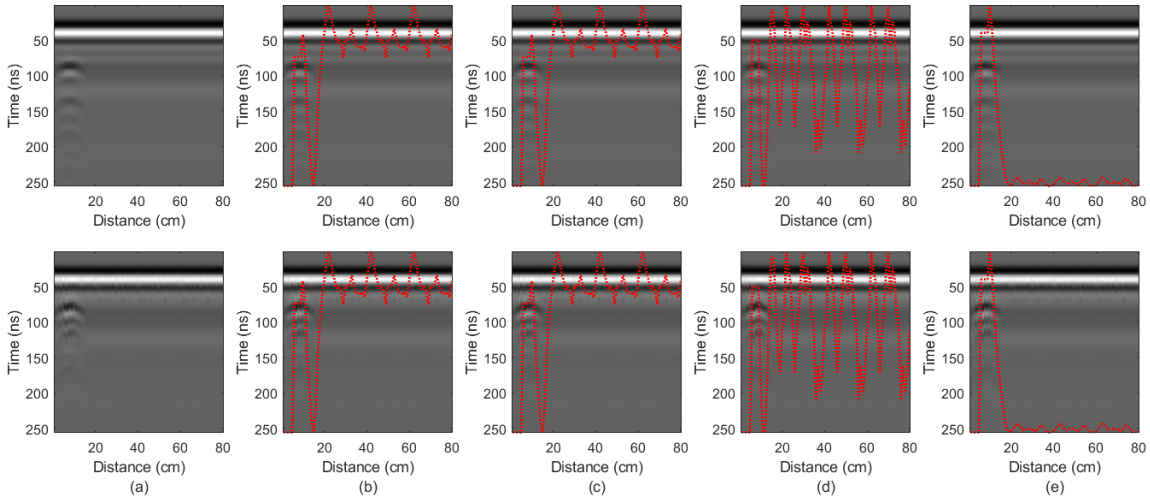

Figure 9. Energy based detection results (first row flat surface, second row rough surface) a) raw data, detection results b) LS c) regLS d) LS_{RPCA}, and e) $regLS_{RPCA}$.

Figure 9 shows the energy based detection results for flat and rough ground surface where the target information is located in the first A-scans. The results of figure 9 (b) and (c) show that Ls and regLs without clutter learning step fail to detect the target, as expected. The Ls_{RPCA} method with clutter learning step also fails as seen in the Figure 9 (c) since the clutter does not vary too much in the simulated dataset and Ls_{RPCA} method encounters a singularity problem in the matrix inversion operation. On the other hand, $regLS_{RPCA}$ successfully detects the target. The pre-processing step provides the clutter part and the regularization step helps to avoid singularity problem. For the simulated dataset, the proposed $regLS_{RPCA}$ method outperforms the others.

The running-time of the cascaded methods are also compared and the results show that all are fast enough for real-time implementation as presented in Table 2. Thus proposing these additional stage does not bring extra burden to the classical LS method [2].

Table 2. Running time comparison of the methods.

Algorithms	SVD	PCA	ICA	NMF	RPCA
Time (s)	0.01	0.01	0.16	0.07	0.10

4.2. Real Dataset Results

Two different real dataset are used for the performance analysis of the proposed method. The first real GPR data is from Vrije Universiteit Brussel [17]. This GPR data contains 4 different targets which are PMA-3, PMA-1, stone and copper strip buried from left to right as shown in Figure 10. There are some irregularities on the surface of the ground around 10 cm and the soil type is dry clay soil mixed with small rocks. The target signature is barely observed in the GPR image.

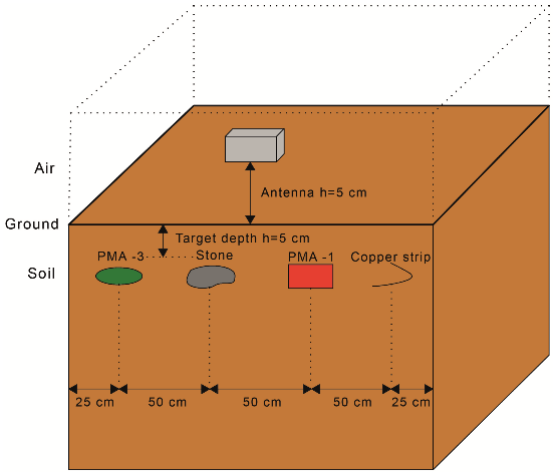

Figure 10. Experimental design of the first real dataset.

The second real GPR data is obtained from landmine clearance operations conducted in Germany as a project of the International Test and Evaluation Program for Humanitarian Demining (ITEP) in 2009 [18]. It contains 5 PPM-2 landmines which are buried in different depths as given in Figure 11 and the soil type is magnetic sand. This real GPR data also contains noise inherently thus it is expected that it will show the superior performance of the proposed method.

As seen in the Figure 12 (a) and (b), the classical and regularized LS methods fail for the first target since the observed A-scans belong to the first target and they also fail to detect the second target.

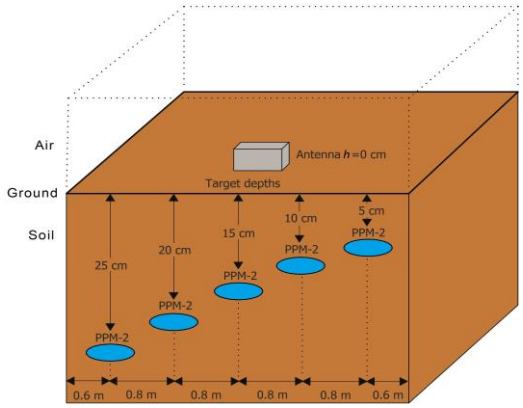

Figure 11. Experimental design of the second real dataset.

The third and the last target are detected. The results in Figure 12 (c) and (d) look similar, both methods detect the first and second targets, validating the effectiveness of the proposed clutter learning preprocessing. To highlight the results, the detection threshold is plotted with green dotted line and proposed method is able to detect 4 targets while LS and regLS fail. They also contain false alarms which is not desired. Besides, the error plot of $regLS_{RPCA}$ is smoother compared to LS_{RPCA}. The obtained results are in accordance with Figure 8 where ROC curves show less FAR ratios.

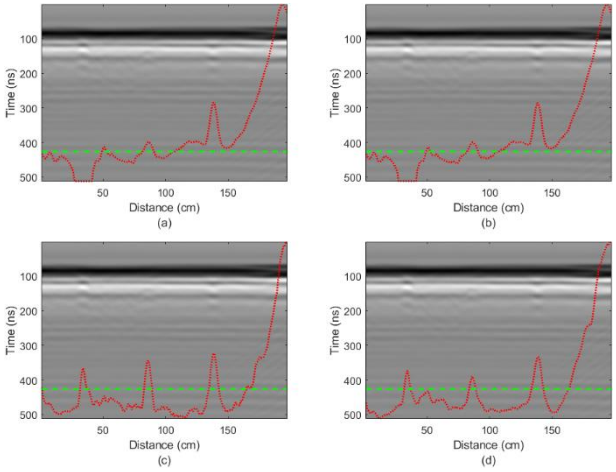

Figure 12. Performance comparison of the methods for the first real dataset a) LS b) regLS c) LS_{RPCA}, and d) $regLS_{RPCA}$.

Figure 13 (a) and (b) show results without clutter removal thus they are not satisfactory for both LS and regLS. Figs 13 (c) and (d) show that the 1st target missed in Figure 13 (a) and b) is detected. The 4th target energy level is higher for $regLS_{RPCA}$ compared to LS_{RPCA}. The proposed method succesfully detects all five targets. Thus, for the real data cases we can conclude that the proposed method outperforms the classical LS method.

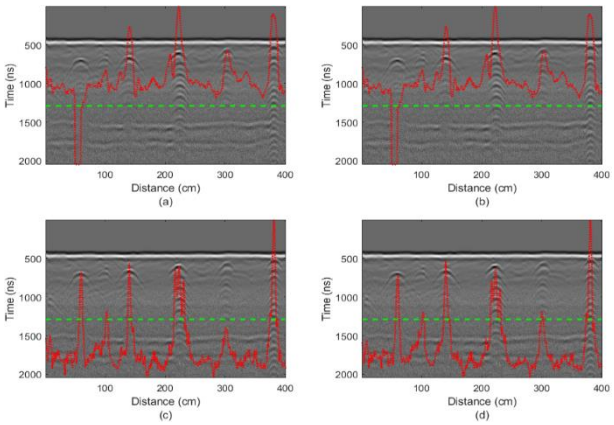

Figure 13. Performance comparison of the methods for the second real dataset a) LS b) regLS c) LS_{RPCA}, and d) $regLS_{RPCA}$.

5. CONCLUSIONS

The conventional LS based GPR target detection method has two drawbacks:

- The classical LS solution deteriorates when the deterministic correlation matrix of the input data is ill-conditioned which frequently occurs when the measurement data is noisy due to rough soil surface,
- It is assumed that the first A-scans which are used to model the clutter do not contain any target information. If this information does not hold (a common case for fields studies), the clutter can not be modelled properly and the resulting model error does not provide an accurate detection result.

To deal with these issues a new 2 stage detection method is proposed. First the clutter is learned using subspace-based methods. Then the learned clutter is used alongside regLS. The conducted experiments for both simulated and real datasets show that the proposed regLS method with clutter learning preprocessing step provides better detection results compared to the classical LS approach. As a future goal, new clutter removal methods can be used in the preprocessing step.

6. REFERENCES

[1] D. J. Daniels, *Ground Penetrating Radar*. IEE, London, U.K. (2004).

[2] A.B. Yoldemir, and M. Sezgin, "A least squares approach to buried object detection using ground penetrating radar." *IEEE Sensors Journal*, Vol. 11, No. 6, pp. 1337-1341, 2011.

[3] E. Temlioglu, I. Erer and D. Kumlu, "A least mean square approach to buried object detection in ground penetrating radar," In *IEEE International Geoscience and Remote Sensing Symposium (IGARSS)*, pp. 4833-4836, July 2017.

[4] B.P.A. Rohman and M. Nishimoto, "GPR Target Signal Enhancement Using Least Square Fitting Background and Multiple Clustering of Singular Values," *Progress In Electromagnetics Research*, Vol. 83, pp.123-132, 2019.

[5] X. Song.; D. Xiang; K. Zhou and Y. Su, "Improving RPCA-based clutter suppression in GPR detection of antipersonnel mines." *IEEE Geosci. Remote Sens. Letters*, Vol. 14, No. 8, pp. 1338-1342, 2017.

[6] F. Abujarad, *Ground Penetrating Radar Signal Processing for Landmine Detection*, PhD Thesis, Otto-Von-Guericke University Magdeburg, Germany (2007).

[7] P.K. Verma, A. N. Gaikwad, D. Singh et al. "Analysis of clutter reduction techniques for through wall imaging in UWB range." *Progress In Electromagnics Res B.*, Vol. 17, pp. 29-48, 2009.

[8] D. Kumlu and I. Erer, "Clutter Removal Techniques in Ground Penetrating Radar for Landmine Detection: A Survey." *In Operations Research for Military Organizations*, IGI Global, pp. 375–399, 2019.

[9] D. Kumlu and I. Erer, "A comparative study on clutter reduction techniques in GPR images." *In* International Conference on Electrical and Electronics Eng., pp.23–328, April 2017.

[10] D. Kumlu and I. Erer, "Clutter removal in GPR images using nonnegative matrix factorization," *Journal of Electromagnetic Waves and Applications*, Vol. 32, No. 16, pp. 2055–2066, 2018.

[11] M. P. Masarik, J. Burns; B. T. Thelen; J. Kelly and T. C. Havens, "GPR anomaly detection with robust principal component analysis." *In* Detection and Sensing of Mines, Explosive objects, and Obscured targets XX, May 2015.

[12] L. Liu, Q. Chen, Y. Han, H. Xu, J. Li, and B. Wang, "Improved Clutter Removal by Robust Principal Component Analysis for Chaos Through-Wall Imaging Radar." *Electronics*, Vol. 9, No. 1, pp .25, 2020.

[13] H. Abdi, *The Method of Least Squares. Thousand Oaks*, CA: Sage, 2010.

[14] D. Kumlu and I. Erer, "Combining Clutter Learning with LS for Improved Buried Target Detection in GPR." *In 9th International Conference on Recent Advances in Space Technologies (RAST)*, pp. 607-611, June 2019.

[15] E. J. Candès, X. Li; Y. Ma and J. Wright, "Robust principal component analysis?." *Journal of the ACM*, Vol. 58, No. 1, pp. 1-37, 2009.

[16] Xu, Y., Wu, Z., Xiao, F., Zhan, T. and Wei, Z, "A target detection method based on low-rank regularized least squares model for hyperspectral images." *IEEE Geoscience and Remote Sensing Letters*, Vol. *13, No.* 8, pp.1129-1133, 2016.

[17] C. Warren, A. Giannopoulos and I. Giannakis, "gprMax: Open source software to simulate electromagnetic wave propagation for ground penetrating radar." *Computer Physics Comm*, Vol. 209, pp. 163-170, 2009.

[18] Real GPR data. Vrije Univ. Brussel (VUB), accessed on Sep. 01, 2011. [Online]. Available: http://www.minedet.etro.vub.ac.be

[19] J. Kim, G. Caire and A.F. Molisch, "Quality-aware streaming and scheduling for device-to-device video delivery." *IEEE/ACM Transactions on Networking*, Vol. 24, No. 4, pp. 2319-2331, 2015.

7. VITAE

Dr. Deniz Kumlu

He received the B.S. degree from the Department of Electrical and Electronics Engineering, Turkish Naval Academy, Istanbul, Turkey, in 2007, the M.S. degree from the Ming Hsieh Department of Electrical Engineering, Viterbi School of Engineering, University of Southern California, Los Angeles, CA, USA in 2012, where he studied with the special fellowship granted from the Turkish Naval Forces. The Ph.D. degree from the Department of Electronic and Communication Engineering, Istanbul Technical University, Istanbul, Turkey, in 2019 with best thesis award of the year. He is currently serving as an Asst. Prof. in the Department of Electrical and Electronics Engineering, National Defense University, Naval Academy. His research interests include image processing, signal processing, statistical signal processing and ground penetrating radar.

Dr. Isin Erer

She is an Associate Professor in the Department of Electronics and Communication Engineering, Istanbul Technical University, Istanbul, Turkey. She received his B.Sc., M.Sc. and PhD degree in Electrical and Electronics Engineering from Istanbul Technical University, Istanbul, Turkey. Her research interests include statistical signal processing, image processing for remote sensing, high-resolution radar imaging and ground penetrating radar.